

2 **Preventive training interferes with mRNA-encoding myosin 7 and collagen I**
3 **expression during pulmonary arterial hypertension**

4 **Preventive training in pulmonary arterial hypertension**

5 Thaoan Bruno Mariano¹, Anthony César de Souza Castilho¹, Ana Karenina Dias de
6 Almeida Sabela¹, André Casanova de Oliveira¹, Sarah Santiloni Cury³, Andreo Fernando
7 Aguiar⁴, Raisa de Jesus Dutra Dias⁵, Antonio Carlos Cicogna², Katashi Okoshi², Luis
8 Antonio Justulin Junior³, Robson Francisco Carvalho³, Francis Lopes Pacagnelli^{1,5}.

9 ¹ Postgraduate program in Animal Science, University of Western São Paulo (Unoeste),
10 Presidente Prudente, São Paulo, Brazil.

11 ² Department of Internal Medicine, Botucatu Medical School, Sao Paulo State University,
12 UNESP, Sao Paulo, Brazil.

13 ³ Department of Structural and Functional Biology, Institute of Biosciences, São Paulo
14 State University, Botucatu, Brazil.

15 ⁴ Postgraduate Program in Physical Exercise in Health Promotion, Northern University of
16 Paraná, Londrina, PR - Brazil

17 ⁵ Department of Physiotherapy, University of Western São Paulo (UNOESTE), Presidente
18 Prudente, SP, Brazil.

19 **Abstract**

20 To gain insight on the impact of preventive exercise during pulmonary arterial
21 hypertension (PAH), we evaluated the gene expression of myosins and gene-encoding
22 proteins associated with the extracellular matrix remodeling of right hypertrophied

23 ventricles. We used 32 male Wistar rats, separated in four groups: Sedentary Control (S;
24 n=8); Control with Training (T; n=8); Sedentary with Pulmonary Arterial Hypertension
25 (SPAH; n=8); and Pulmonary Arterial Hypertension with Training (TPAH; n=8). The rats
26 trained for thirteen weeks on a treadmill. They had two weeks of adaptation training. The
27 PAH was induced by application of monocrotaline 60 mg/kg. Consequential right
28 ventricular dysfunction was observed after the 10th week of training. Rats in the control
29 group received saline application. At the end of the 13th week, echocardiography analysis
30 confirmed cardiac dysfunction. Collagen content and organization was assessed through
31 picrosirius red staining and fractal dimension (FD) analysis, respectively. Transcript
32 abundance was estimated through reverse transcription-quantitative PCR (RT-qPCR).
33 Cardiac dysfunction was confirmed by the reduction in maximum pulmonary artery
34 velocity and pulmonary artery acceleration time. Through histomorphometric
35 assessment, we found no differences in the interstitial collagen FD between groups.
36 Regarding gene expression, *myh7* gene expression was upregulated in the TPAH group.
37 However, this did not occur with the S group. PAH also increased the mRNA abundance
38 of *coll1a1* in the SPAH and TPAH groups. Moreover, the TPAH group showed a higher
39 abundance of this gene when compared to the S group. With these findings, we concluded
40 that preventive exercise had a positive impact on compensated hypertrophy during
41 pulmonary hypertension. This can be explained in part by the modulation of the
42 extracellular matrix and myosin gene expression in trained rats.

43 **Introduction**

44 Pulmonary Arterial Hypertension (PAH) is a severe and disabling disease that
45 causes right ventricular (RV) remodeling. This is shown by compensatory hypertrophy
46 and subsequent right ventricular heart failure (HF), the latter being the main prognostic
47 determinant and common cause of death [1]. Alterations in myosin and extracellular

48 matrix-related genes are possible mechanisms involved in the PAH cardiac hypertrophy
49 phase. A study of the HF phase in isolated right ventricular myocytes using monocrotaline
50 demonstrated a reduction in ATPase activity in the myosin head [2]. These changes in
51 myosin heavy chains are critical in the different forms of HF. The chains are the main
52 contractile proteins of the heart, and alterations can directly lead to decreased myocardial
53 contractility [2, 3].

54 Cardiac collagen increases have been shown in other studies that used
55 monocrotaline for induced right ventricular HF [4]. Cardiac collagen increases have been
56 associated with different forms of overload pressure and increases to myosin with lower
57 ATPase capacity [3]. Right ventricular failure is characterized by extensive fibrosis and
58 changes to extracellular matrix protein expression, collagen, and metalloproteinases [5].
59 However, the genetic expressions of myosins, collagen, and metalloproteinases have not
60 been studied in the compensatory hypertrophy phase of PAH [5].

61 Exercise is a commonly-used approach to control and limit cardiac damage. It
62 promotes changes in cardiac remodeling and shows benefits in human and animal models
63 with RV hypertrophy [6,7]. Preventive exercise promotes a cardioprotective effect on
64 PAH, as it improves RV function and softens the evolution of the pathological cardiac
65 remodeling process [8,9]. Various molecular mechanisms have been studied to evaluate
66 cardiac functional improvement from preventive training. These mechanisms include the
67 expression of calcium transit genes, regulation of TNF superfamily cytokines, and the
68 quantification of myosin isoforms. However, the effects of changes to the extracellular
69 matrix gene expression and myosins on PAH have not been explored. In the HF phase,
70 pathological remodeling is impossible to reverse by therapy. Thus, approaches to treat
71 compensatory hypertrophy are important to alleviate dysfunctional impairment [10].

72 PAH-compensated right ventricular hypertrophy often evolves to HF and results
73 in high death rates and frequent hospitalizations. This validates the necessity of
74 elucidating effects of preventive training and molecular mechanisms on right ventricular
75 hypertrophy, as this phase precedes HF. This study hypothesizes that preventive aerobic
76 training mitigates the gene changes in the compensated ventricular hypertrophy phase in
77 monocrotaline-induced PAH rats. The study investigates the influence of preventive
78 aerobic training in rats with compensated right ventricular hypertrophy on the gene
79 expression of myosin heavy chains and the extracellular matrix.

80 **Materials and methods**

81 **Ethical approval**

82 The experimental protocols used in this study were approved by the Animal
83 Experimentation Ethics Committee (CEUA) from the University of Western São Paulo,
84 Presidente Prudente, São Paulo, Brazil (Protocol numbers 2483 and 2484). The rats
85 received care following the "Laboratory Animal Care Principles" formulated by the
86 National Society for Medical Research and the Guide for the Care and Use of Laboratory
87 Animals, prepared by the Laboratory Animal Research Institute [11].

88 **Experimental groups**

89 To conduct this study 32 male Wistar rats were used, 2 months of age and average weight
90 of 205 ± 17.43 g, from the Central Animal Facility of the University of Western São Paulo,
91 UNOESTE. All animals were housed in a room under temperature control at 23 °C,
92 relative humidity of 50–60%, and kept on a 12-hour light/dark cycle. Food and water
93 were supplied *ad libitum*.

94 The animals were randomly distributed into four experimental groups of eight animals
95 each, denominated as Sedentary Control (S; n=8); Control with Training (T; n=8);

96 Sedentary with Pulmonary Arterial Hypertension (SPAH; n=8); and Pulmonary Arterial
97 Hypertension with training (TPAH; n=8).

98

99 **Preventive Training**

100 Rats from the T and TPAH groups were submitted to an adapted treadmill aerobic
101 training protocol (model TK 1, IMBRAMED). The protocol consisted of 13 total weeks,
102 five days a week. The first two weeks were for adaptation (pre-training). After, the rats
103 performed the exercises for eight weeks, with gradual increases in intensity, as described
104 previously. The rats were then injected with monocrotaline or saline and performed the
105 exercises for three more weeks. [12, 13].

106 **Incremental exercise test**

107 The rats in the T and TPAH groups were submitted to incremental stress tests.
108 These were performed 24 hours after monocrotaline administration and at the start of the
109 11th, 12th, and 13th weeks to adjust the exercise speed [13, 14]. All exercise was
110 performed with 0% slope. The tests began with a warm-up at 0.5 km/h, followed by five
111 minutes of rest. The speed was then increased to 0.7 km/h for three minutes, followed by
112 increases of 0.2 km/h every three minutes until lactate reached a 1 mmol/l comparative
113 value or exhaustion [15]. Exhaustion was defined as the moment when rats could not
114 continue running for three consecutive minutes. After each increased load, the rats were
115 manually removed from the exercise area for one minute for blood collection. Blood
116 samples were taken from rat tails every three minutes. We used an Accutrend Plus
117 lactometer (Roche, Barcelona, Spain). The device was calibrated to the manufacturer's
118 specifications. The calculation for stipulating maximum velocity was performed using
119 the arithmetic mean of all experimental group velocities until lactate threshold or
120 exhaustion [16]. Lactate threshold was defined as the rate of rotation without a lactate

121 increase of 1.0 mmol/l above the blood-lactate concentration [12,17]. We used an adapted
122 version of the protocol created by Carvalho *et al.* [15].

123 **Echocardiographic evaluation**

124 Echocardiographic evaluation was performed using an echocardiogram (General
125 Electric Medical Systems, Vivid S6, Tirat Carme, Israel) equipped with a 5-11.5 MHz
126 multifrequency probe. The rats were intraperitoneally anesthetized with ketamine (50mg
127 kg⁻¹; Dopalen®) and xylazine (0.5 mg kg⁻¹; Anasedan®).

128 The following LV variables were measured: diastolic (LVDD) and systolic
129 (LVSD) diameters, ratio of E and A waves (E/A), percentage of endocardial shortening
130 (EFS), isovolumetric relaxation time (IVRT), heart rate frequency (HR), ejection fraction
131 (EF), and posterior wall shortening velocity (EPVP). The following RV variables were
132 measured: pulmonary artery flow obtained by doppler, maximum flow velocity time
133 [Acceleration time velocity (PVAT)], pulmonary ejection time (PET), and peak flow
134 velocity (PVF) [12, 18, 19]. Pulmonary velocity acceleration time is an indicator of the
135 severity of pulmonary hypertension. Increases to pulmonary systolic blood pressure
136 levels correspond to decreases in PVAT values. Pulmonary ejection time is a parameter
137 related to systolic function and the degree of PAH. Maximum flow velocity is related to
138 RV systolic function [12, 20, 21].

139 **Euthanasia**

140 After the echocardiographic evaluation (48 hours), the rats were weighed and then
141 euthanized with an intraperitoneal dose of sodium pentobarbital (50 mg/kg). At
142 euthanasia two observers determined the presence or absence of clinical and
143 pathological congestive heart failure features. The clinical finding suggestive of
144 heart failure was tachypnea/labored respiration. Pathologic assessment of cardiac

145 decompensation included subjective evaluation of pleuropericardial effusion, atrial
146 thrombi, ascites, and liver congestion.

147 **Evaluation of anatomical parameters**

148 The heart was removed, dissected into the atria (AT), right ventricles (RV) and left
149 ventricles (LV) and ventricular septum and weighed. The anatomical parameters were
150 normalized by the final body weight (AT/FBW, RV/FBW and LV/ FBW) and were used
151 as the hypertrophy index. The lungs and liver were also removed, weighed and stored in
152 an oven for 48 h. Next, they were weighed again to calculate the wet/dry weight ratio
153 which was used to evaluate signs of cardiac failure [15].

154 **Histology and fractal analysis**

155 The right ventricle was divided into two parts. One part was fixed in 10% buffered
156 formalin solution for 48 hours, and the other was used for gene expression analysis. After
157 fixation, the tissues were placed on paraffin blocks. Coronal histological sections were
158 viewed using a Leica microtome (RM 2155). The histological sections were stained on
159 slides with haematoxylin–eosin solution (HE) to measure the cross-sectional areas of the
160 cardiomyocytes, using a LEICA microscope (model DM750, Leica Microsystems,
161 Wetzlar, Germany). At least 50 cardiomyocyte diameters were measured from each RV
162 as the shortest distance between borders drawn across the nucleus.

163 Histological sections of the RV myocardial interstitium were stained on
164 histological slides by the Picrosirius technique for collagen visualization. The cardiac
165 tissue images were captured by a computer coupled to a camcorder. Digital images from
166 the LEICA DM LS microscope (model DM750, Leica Microsystems, Wetzlar, Germany)
167 were sent to a computer equipped with Image-Pro Plus (Media Cybernetics, Silver Spring,
168 U.S.). The red collagen color (picrosirius) were turned blue to reveal the percentage of
169 collagen in relation to the total area of the image. Twenty fields of each right ventricle

170 were analyzed using a 40X objective with 400x magnification. The chosen fields were
171 far from the perivascular region [22].

172 Binarized photographs and the box-counting method using ImageJ software were
173 used for FD analysis. The software used box-counting with two dimensions. This allowed
174 for the quantification of pixel distribution without interference from the texture of the
175 image. This results in two images (binarized and gray level) with the same FD. The
176 analysis of the fractal histological slides was based on the relation between the resolution
177 and the evaluated scale. The result was quantitatively expressed as the FD of the object
178 with $DF = \frac{1}{4} (\log N_r / \log r_{-1})$; N_r as the quantity of equal elements needed to fill the
179 original object with scale applied to the object). FD was calculated using the ImageJ
180 software set between 0 and 2, without distinguishing different textures [23, 24, 25].

181

182 **Real-time polymerase chain reaction after reverse transcription (RT-qPCR)**

183 Total RNA was extracted from RV tissue using TRIzol (ThermoScientific,
184 Waltham, U.S.) and then treated with DNase deoxyribonuclease I (ThermoScientific)
185 following the manufacturer's instructions. RNA integrity was evaluated by agarose gel
186 electrophoresis for visualization of ribosomal RNAs. The High Capacity Reverse
187 Transcriptional Kit (ThermoScientific) was used for the synthesis of complementary
188 RNA (cDNA) from 1000 ng of total RNA for each sample. Using real-time quantitative
189 PCR (qPCR), cDNA was used to evaluate the relative levels of *Rattus norvegicus* myosin
190 heavy chain 7 (*myh6*) mRNA, *Rattus norvegicus* myosin heavy chain 7 (*myh7*), *Rattus*
191 *norvegicus* myosin heavy chain 7B (*myh7b*), *Rattus norvegicus* collagen type I alpha 1
192 chain (*coll1a1*) mRNA, *Rattus norvegicus* collagen type I alpha 2 chain (*coll1a2*), *Rattus*
193 *norvegicus* collagen type 3 alpha 1 chain (*col3a1*) mRNA, and *Rattus norvegicus*
194 metalloproteinases 2 (*mmp2*) mRNA. The Taqman™ Universal Master Mix II

195 (Applied Biosystems, Foster City, U.S.) and the StepOne Plus system (ThermoScientific)
196 were used for qPCR. All samples were analyzed in duplicates. The cycling conditions
197 were at 50 °C for two minutes and 95 °C for 10 minutes. This was followed by 40 cycles
198 of denaturation at 95 °C for 15 seconds and the final extension at 60 °C for one minute.
199 Gene expression was quantified relative to the values of the S group after normalization
200 by expression levels of the beta-actin reference gene (*Actb*) using the 2^{-DDCt} method
201 [26]. Primer sequences were selected from GenBank transcript access numbers
202 (<http://pubmed.com>) and designed using Primer Express v.3.0 software
203 (ThermoScientific).

204 **Data analysis**

205 Statistical analyses were performed using GraphPad Prism software (Graph-Pad
206 Software, La Jolla, U.S.). The Shapiro-Wilk test was used to assess data normality. To
207 analyze the echocardiogram data, Kruskal-Wallis test and Dunn's post test were used with
208 data from the collagen interstitial fraction and the expression of myh6 and *colla1* mRNA.
209 ANOVA and Tukey's post test were used with data from the expression of myh7 and
210 *colla2* mRNA. Data were expressed with box plot graphs that showed the first and third
211 quartile, median, minimum, and maximum. The significance level was considered when
212 $p < 0.05$.

213 **Results Echocardiographic evaluation**

214 The LV echocardiographic evaluation is presented in Table 1. LVDD was lower
215 in the SPAH group when compared to rats in the control group. LVDD was higher in the
216 T group when compared to rats in the control group. The rats treated with monocrotaline
217 presented RV dysfunction due to the decrease in the maximum pulmonary artery velocity

218 (Vmax-Pulm) and the pulmonary artery acceleration time (TAC-pulm). An improvement
219 of VMmax-Pulm in the TPAH group was recorded (Figure 1).

220

221 Table 1. Left ventricle echocardiographic evaluation.

PARAMETERS	S (n=8)	SPAH (n=8)	T (n=8)	TPAH (n=8)
HR (bpm)	310.71±46.58	331.66±35.65	314±38.25	325.44±42.81
LVDD (mm)	7.84±0.54	7.02±0.73*	8.25± 0.50*	7.37±0.94
LVSD (mm)	4.14±0.48	3.59±0.47	4.39± 0.39	3.45±0.81
EFS	47.33±3.56	48.72± 6.05	46.86± 2.28	53.50± 7.07
E/A	1.55± 0.31	1.07±0.36	1.37± 0.19	1.12± 0.37
PWSV (mm/s)	34.21±0.90	37.37± 3.43	37.85± 3.30	37.38±3.85
IVRT (ms)	22.57± 3.59	31.55± 9.40	22± 3.57	28.66±7.26
Ejection Fraction	0.85±0.030	0.86±0.048	0.84±0.019	0.89±0.043

222 Data are expressed as mean ± standard deviation. Heart rate (HR), diastolic
223 (LVDD) and systolic (LVSD) diameters, percentage of endocardial shortening (EFS), the
224 ratio of E and A waves (E/A), posterior wall shortening velocity (PWSV), time
225 isovolumetric relaxation rate (IVRT), ejection fraction (EF). S (n=8): Sedentary Control;
226 T (n=8): Control with Training; SPAH (n=8): Sedentary Pulmonary Arterial
227 Hypertension; TPAH (n=8): Pulmonary Arterial Hypertension with Training.

228 * Statistical difference $p < 0.05$.

229

FIGURE 1

230 Figure 1. RV echocardiographic evaluation presented in a boxplot. A. PVAT: pulmonary
231 velocity acceleration time; B. PET: pulmonary artery ejection time; C. PVF: peak flow
232 velocity of the pulmonary artery. S (n=8): Sedentary Control; T (n=8): Control with
233 Training; SPAH (n=8): Sedentary Pulmonary Arterial Hypertension; TPAH (n=8):
234 Pulmonary Arterial Hypertension with Training.

235 **Group characterization and anatomic parameters**

236 In PAH (n=16), all rats presented right ventricular and atria hypertrophy (S= $0,22 \pm$
237 $0,03$ g; SPAH= $0,37 \pm 0,18$ g; TPAH= $0,36 \pm 0,19$ g, $p < 0,05$). There was no clinical or
238 pathological evidence of heart failure.

239 **Histological and fractal analysis**

240 Fiber cross sectional areas were higher in PAH groups (S= $62,39 \pm 6,37$ μm^2 ;
241 SPAH: $104,88 \pm 21,83$ μm^2 ; TPAH= $89,23 \pm 7,99$ μm^2 , $p < 0,05$). Comparisons between
242 rats that performed preventive exercise and sedentary rats did not show statistical
243 difference ($p > 0.05$) in the percentage of cardiac interstitial collagen (Figure 2) and fractal
244 analysis (Figure 3).

245

FIGURE 2

246 Figure 2. Absence of impact of preventive exercise on cardiac interstitial collagen fraction
247 in PAH. Cross-sections of the cardiac muscle were stained by the Picrosirius Red
248 technique and viewed with 40x objective and 400x magnification. Groups A. S (n=8):
249 Sedentary Control; B. T (n=8): Control with Training; SPAH (n=8): Sedentary
250 Pulmonary Arterial Hypertension; TPAH (n=8): Pulmonary Arterial Hypertension with
251 Training.

252

FIGURE 3

253 Figure 3. Fractal dimension analysis of right ventricle tissue stained with the Picrosirius
254 Red technique and viewed with 40x objective and 400x magnification.

255

256 **Relative gene expression**

257 Preventive exercise increased the *Myh7* expression gene in the TPAH group when
258 compared to the control group (S vs. TPAH, $p = 0.0242$). The expression of *colla1* was
259 higher in the groups with PAH when compared to the sedentary and trained groups (S vs.
260 SPAH, S vs. TPAH, T vs. TPAH, $p = 0.0008$). The other groups did not present
261 statistically significant differences (Figure 4).

262

FIGURE 4

263 Figure 4. The mRNA abundance of A. *Myh6* gene expression. B. *Myh7* gene expression.
264 C. *Myh7b* gene expression. D. *Colla1* gene expression. E. *Colla2* gene expression. F.
265 *Col3a1* gene expression. G. *Mmp2* gene expression in right ventricle of experimental
266 groups. S (n=8): Sedentary Control; T (n=8): Control with Training; SHAP (8): Sedentary
267 Pulmonary Arterial Hypertension; TPAH (n=8): Pulmonary Arterial Hypertension with
268 Training. * Statistical difference $p < 0.05$.

269 **Discussion**

270 The main finding of the current study was that preventive physical exercise
271 increased *myh7* and *colla* in the PAH-compensated ventricular hypertrophy phase. This
272 interfered in disease progression. Despite persistent right pressure overload,
273 echocardiography confirmed an increase in cardiac function.

274 Myosins are the major contractile proteins of muscle. In the heart, there are heavy
275 myosin chains (α -MHC and β -MHC), regulatory light myosin chains, and essential light
276 chain protein C-linked myosin [23, 27]. A-MHC has a higher sliding speed and two to
277 three times higher ATPase activity than β -MHC; but β -MHC can generate force with
278 lower energy expenditure [28]. Our results showed an increase in the *myh7* gene
279 responsible for the β -MHC protein in rats from the PAH preventive exercise group.

280 The increase in the *myh7* gene may be a compensatory mechanism in the PAH
281 exercise group. The increase of this specific myosin is typically related to poorly adaptive
282 cardiac remodeling [29]. However, our study showed that this increase came with cardiac
283 function improvements. A study from Moreira-Gonçalves *et al.* 2015 [4] also showed an
284 increase of myosin in an exercise-performing group that was without weakened
285 ventricular function. Another study showed that rats with HF (from isoproterenol)
286 preserved cardiac function with increased *myh7* and reduced *myh6* [29].

287 Early expressed transcription factors are other mechanisms that relate to the
288 regulation of MHC genes. These include GATA transcription factor 4, NK2 homeobox 5
289 (*Nkx2-5-gene*), MADS-box transcription factor, serum response factor (Srf) (attenuates
290 the expression of *myh6* and *myh7*), myocyte enhancer factor 2 (MEF2) and AT, factors
291 that bind to the Mcat malonyl-CoA-acyl carrier protein transacylase sequence, and
292 forkhead box O1 (Foxo1). Foxo1 can act as an *myh6* repressor through histone
293 deacetylase or the N-CoR nuclear suppressor [30]. A purine-rich negative regulatory
294 (PNR) element is present in the first region of the *myh6* gene. When increased, it reduces
295 the expression of this myosin by 20 to 30 times [31, 32]

296 In addition to myosins, there is a cardiac collagen network that supports and
297 connects all structures and assists inadequate cardiac function (systolic and diastolic). The

298 network has a fundamental role in resisting pathological deformations, maintaining
299 structural alignment, regulating distensibility, and forcing transmission during cardiac
300 fiber shortening [7, 33, 34]. In our study, the phase of cardiac dysfunction by PAH
301 increased *coll1a1* gene expression, demonstrating the role of this gene in the worsening
302 of cardiac functionality.

303 Collagen content and organization were unaltered in our study. FD is a useful
304 method for assessing the organization via images from fractals. These images reveal the
305 amount of space and self-similarity of the structure, detect subtle morphological changes,
306 and perform functional quantitative measurements [25]. Despite alterations to gene
307 expression, fractal evaluation showed that tissue collagen organization was preserved.

308 In pathological situations, such as acute myocardial infarction and pressure
309 overload, one study showed that increased interstitial fibrosis directly relates to the
310 worsening of ventricular contractile function [34]. The authors of this study also used
311 echocardiography to demonstrate the worsening of contractile function. Size increases to
312 the septal thickness, LV posterior wall, and chamber were observed and associated with
313 reduced ejection fraction and increased diastolic pressure.

314 In different forms of HF, the gene expressions of *coll1a1*, *coll1a2*, and *col3a1*
315 increase due to pressure overload or infarction. However, quantity depends on the cause
316 of HF [34-37]. With pressure overload, an increase of type 1 collagen leads to cardiac
317 stiffness. This occurs from diastole and systole alterations, loss of control in structure
318 alignment, and the regulation of cardiac distensibility and force transmission [7, 33, 34].

319 Cardiac collagen is altered by pressure overloads from mechanical stress-
320 activating fibroblasts. This induces an inflammatory process through concomitant
321 increases in the extracellular matrix [38]. In the monocrotaline PAH model, pressure

322 overload is from increased pulmonary vascular resistance, with activation of the NF- κ B
323 pathway [8]. Our study shows these changes may cause an early increase of the *coll1a1*
324 gene.

325 In response to an injury, the cardiac extracellular matrix assists in electrical and
326 chemical signals, provides structural support, and facilitates mechanical signals. The
327 matrix has metalloproteinases that play an important role in several cardiac pathologies,
328 including dilated cardiomyopathy, myocardial infarction, and hypertensive cardiac
329 hypertrophy [39]. MMPs 2 and 9 cause damage to cardiomyocytes when increased. This
330 leads to the worsening of the cardiac muscle and HF [39]. We did not find the expected
331 increase in MMP2 in the groups with PAH. This factor may have contributed to cardiac
332 function preservation.

333 Rats with aortic constriction have demonstrated greater increases in the *coll1a1*
334 gene when compared to *col3a1* [35]. In acute myocardial infarction, the *col3a1* gene
335 increases more than *coll1a1*. This is a consequence of the cardiac tissue healing process
336 [34]. One study demonstrated that both types of collagen genes can be attenuated by post-
337 transcriptional inhibition from miR-29b microRNA. In addition, aerobic training alters a
338 set of microRNAs associated with improved heart function [39]. For the hypertension
339 group in our study, increases to *coll1a1* gene expression and functional worsening were
340 recorded. This gene continued to increase in the exercise group, and functional
341 improvements were recorded. Other cardioprotective factors released in the myocardium
342 from exercise could have neutralized these adverse aspects of cardiac remodeling. These
343 include the expression of genes that control the transport of calcium, regulate TNF
344 superfamily cytokines, improve oxidative function [4, 8], and have anti-fibrotic effects
345 for inflammatory process reduction [40].

346 Physical exercise is used as a non-pharmacological approach for PAH. Exercise
347 is performed for cardiopulmonary rehabilitation of the disease. However, exercise as a
348 preventive approach for right ventricular dysfunction has not been thoroughly researched
349 [8, 13]. In our study, *myh7* and *coll1a1* genes increased and cardiac function improved
350 (observed by echocardiography) after preventive exercise on a treadmill for up to 60
351 minutes, five days a week for 13 weeks, at speeds until 1.1 km/h [13]. Additional
352 molecular mechanisms should be studied to demonstrate improvements from exercise in
353 the early phase of PAH.

354 Beneficial influences of various types of exercise on myosin and cardiac collagen
355 have already been demonstrated. Aerobic exercise induces physiological cardiac
356 hypertrophy from the volume load imposed on the heart without rest periods. This results
357 in increased biosynthesis of contractile components, including increases to fast myosin
358 heavy chains (α -MHC) and decreases to slow isoforms (β - MHC) [41].

359 Regarding collagen, SOCI *et al.* [42] demonstrated that swimming increases
360 miRNA-29c expression in healthy rats, reducing the expression of cardiac collagen genes
361 *coll1a1* and *col3a1*. Another study showed rats with cardiac abnormalities from aging
362 reduced fibrosis and *colla2* after exercise on the treadmill for 12 weeks [43]. For acute
363 myocardial infarction, exercise on the treadmill with a moderate inclination of 5° for 45
364 minutes reduced *colla2* and *col3a1* [44]. In rats six weeks after acute myocardial
365 infarction, resistance exercise four times a week with 75% of 1RM with 10-12 repetitions
366 combined with treadmill exercise five times a week at 15 meters/minute for 12 weeks
367 improved the interstitial collagen fraction due to the effect of pathological hypertrophy
368 reversal [45, 46]. However, increased interstitial collagen was not observed in our study.
369 The increase in the *coll1a1* gene may indicate that collagen increases later and affects

370 cardiac dysfunction. Similar to myosins, collagen may be influenced by exercise
371 modality, frequency, duration, intensity, and the disease phase when training starts [8].

372 We conclude from our findings that preventive exercise is beneficial for
373 compensated hypertrophy in pulmonary hypertension. This could be partially explained
374 by the modulation of the extracellular matrix and myosin gene expression in exercise
375 group rats. Other mechanisms, pathways, and variations in exercise intensity and type
376 should be investigated in the preclinical PAH phase.

377 Lastly, our findings showed that exercise yielded benefits when started before
378 and in the early stages of the disease. This confirmed the importance of exercise as a
379 preventive approach provides considerable cardioprotection against the deleterious
380 effects of PAH, which reinforces the importance of maintaining a physically active
381 lifestyle. Clinical trials that examine effects of exercise on PAH should use individuals
382 with the early stage of the disease.

383 **Acknowledgments**

384 We would like to thank Eric Schloeffel for his help with English editing.

385 **References**

- 386 1 Humbert M, Guignabert C, Bonnet S, et al. Pathology and pathobiology of pulmonary
387 hypertension: state of the art and research perspectives. *Eur Respir J.* 2019; 53: 1801887
- 388 2 Vescovo G, Jones SM, Harding SE & Poole-wilson PA. Isoproterenol sensitivity of
389 isolated cardiac myocytes from rats with monocrotaline-induced right-sided hypertrophy
390 and heart failure. *J Mol Cell Cardiol.* 1989; 21: 1047-61.

- 391 3 Batlle M, Castillo N, Alcarraz A, et al. Axl expression is increased in early stages of
392 left ventricular remodeling in an animal model with pressure-overload. *PLoS One*.
393 2019;14(6): e0217926.
- 394 4 Moreira-Gonçalves D, Ferreira R, Fonseca H, et al. Cardioprotective effects of early
395 and late aerobic exercise training in experimental pulmonary arterial hypertension. *Basic*
396 *Res Cardiol*. 2015;110: 57.
- 397 5 Nadadur RD, Umar S, Wong G, et al. Reverse right ventricular structural and
398 extracellular matrix remodeling by estrogen in severe pulmonary hypertension. *J Appl*
399 *Physiol*. 2012; 113: 149–158.
- 400 6 Colombo R, Siqueira R, Becker CU, et al. Effects of exercise on monocrotaline-induced
401 changes in right heart function and pulmonary artery remodeling in rats. *Can J Physiol*
402 *Pharmacol*. 2013; 91: 38-44.
- 403 7 Zile MR, Baicu CF, Ikonomidis J, et al. Myocardial Stiffness in Patients with Heart
404 Failure and a Preserved Ejection Fraction: Contributions of Collagen and Titin.
405 *Circulation*. 2015; 131: 1247-1259.
- 406 8 Nogueira-Ferreira R, Moreira-Gon D, SilvaAna F, et al. Exercise preconditioning
407 prevents MCT-induced right ventricle remodeling through the regulation of TNF
408 superfamily cytokines, *Intern J Cardiol*. 2016; 203: 858–866.
- 409 9 Pacagnelli FL, Aguiar AF, Campos DHS, et al. Training improves the oxidative
410 phenotype of muscle during the transition from cardiac hypertrophy to heart failure
411 without altering MyoD and myogenin. *Exp Physiol*. 2016; 101: 1075–1085.
- 412 10 Gonzalez A, Ravassa S, Beaumont J, Lopez B, Diez J. New targets to treat the
413 structural remodeling of the myocardium. *J Am Coll Cardiol*. 2011; 58: 1833–1843.

- 414 11 Clark J.D., Gebhart G.F., Gonder J.C. et al. (1997) The 1996 guide for the care and
415 use of laboratory animals. *ILAR J.* 38, 41–48.
- 416 12 Lopes FS, Carvalho RF, Campos GE, Sugizaki MM, Padovani CR, Nogueira CR,
417 Cicogna AC, Dal-Pai-Silva M. Down-regulation of MyoD gene expression in rat
418 diaphragm muscle with heart failure. *Int J Exp Pathol.* 2008; 89: 216-222.
- 419 13 Pacagnelli FL, Sabela AK, Okoshi K, et al. Preventive physical training exerts a
420 cardioprotective effect in rats treated with monocrotaline. *Int j Exp Pathol.* 2016; 97: 238-
421 247.
- 422 14 Rodrigues B, Figueroa DM, Mostarda CT, Heeren MV, Irigoyen MC & Angelis K.
423 Maximal exercise test is a useful method for physical capacity and oxygen consumption
424 determination in streptozotocin-diabetic rats. *Cardiovasc diabetol.* 2007; 13: 1-7.
- 425 15 Carvalho JF, Masuda MO & Pompeu FAMS. Method for diagnosis and control of
426 aerobic training in rats based on lactate threshold. *Comp Biochem Physiol A Mol Integr*
427 *Physiol.* 2005; 140: 409–413.
- 428 16 Svedah K & Macintosh BR. Anaerobic threshold: the concept and methods of
429 measurement. *Canad J Appl Physiol.* 2003; 28: 299-323.
- 430 17 Souza RWA, Piedade WP, Soares LC, et al. Aerobic exercise training prevents heart
431 failure-induced skeletal muscle atrophy by anti-catabolic, but not anabolic actions. *PLoS*
432 *One.* 2014; 9: 1-15.
- 433 18 Ferreira JCB, Rolim NPL, Bartholomeu JB, Gobatto CA, Kokubun E & Brum PC.
434 Maximal lactate steady state in running mice: effect of exercise training. *Clin Exp*
435 *Pharmacol Physiol.* 2007; 34: 760-765.

- 436 19 Martinez ST, Santos APB & Pinto AC. A Determinação Estrutural do Alcaloide
437 Pirrolizidínico Monocrotalina: Exemplo dos Desafios da Química de Produtos Naturais
438 Até os Anos Sessenta do Século XX. *Rev Virtual Quim.* 2013; 5: 300-311.
- 439 20 Eguchi M, Ikeda S, Kusumoto S et al. Adipose-derived regenerative cell therapy
440 inhibits the progression of monocrotaline-induced pulmonary hypertension in rats. *Life*
441 *Sci.* 2014; 118: 306-312.
- 442 21 Dabestani A, Mahan G, Gardin JM et al. Evaluation of pulmonary artery pressure and
443 resistance by pulsed Doppler echocardiography. *Am J Cardiol.* 1987; 59: 662–668.
- 444 22 Pacagnelli FL, Okoshi K, Campos DHS, et al. Physical training attenuates cardiac
445 remodeling in rats with supra-aortic stenosis. *Exp Clin Cardiol.* 2014; 20: 3889–3905.
- 446 23 Zornoff LAM, Matsubara BB, Matsubara LS & Minicucci MF. Cigarette smoke
447 exposure intensifies ventricular remodeling process following myocardial infarction. *Arq*
448 *Bras Cardiol.* 2006; 86: 276–282.
- 449 24 Cury SS, Freire PP, Martinucci B, et al. Fractal dimension analysis reveals skeletal
450 muscle disorganization in mdx mice. *Biochem Biophys Res Commun.* 2018; 3; 503
451 (1):109-115.
- 452 25 Fávero PF, Lima VAV, Santos PH, et al. Differential fractal dimension is associated
453 with extracellular matrix remodeling in developing bovine corpus luteum. *Biochem*
454 *Biophys Res Commun.* 2019; 27; 516(3): 888-893.
- 455 26 Livak KJ & Schmittgen KD. Analysis of relative gene expression data using real-time
456 quantitative PCR and the 2^{-ΔΔC(T)} method. *Methods.* 2001; 25, 402-408.
- 457 27 Marsiglia JDC & Pereira AC. Cardiomiopatia Hipertrófica: Como as Mutações Levam
458 à Doença? *Arq Bras Cardiol.* 2014; 102, 295-304.

- 459 28 Cai M, Huang Q, Liao W, Wu Z, Liu F & Gao Y. Hypoxic training increases metabolic
460 enzyme activity and composition of myosin heavy chain isoform in rat ventricular
461 myocardium. *Eur J Appl Physiol*. 2010; 108: 105–111.
- 462 29 Kralova E, Doka G, Pivackova L, Srankova J, et al. L-Arginine Attenuates Cardiac
463 Dysfunction, But Further Down-Regulates α -Myosin Heavy Chain Expression
464 in Isoproterenol-Induced Cardiomyopathy. *Basic & Clin Pharmacol Toxicol*. 2015; 117:
465 251–260
- 466 30 Qi Y, Zhu Q, Zhang K, et al. Activation of Foxo1 by Insulin Resistance Promotes
467 Cardiac Dysfunction and β -Myosin Heavy Chain Gene Expression. *Circ Heart Fail*.
468 2015; 8: 198-208.
- 469 31 Gupta MP. Factors controlling cardiac myosin-isoform shift during hypertrophy and
470 heart failure. *J Mol Cell Cardiol*. 2007; 43: 388-403.
- 471 32 Giger JM, Bodell PW, Baldwin KM, Haddad F. The CAAT-binding transcription
472 factor 1/nuclear factor 1 binding site is important in β -myosin heavy chain antisense
473 promoter regulation in rats. *Exp Physiol*. 2009; 94: 1163–1173.
- 474 33 Shoulders MD & Raines RT. Collagen structure and stability. *Annu Rev Biochem*.
475 2009; 78: 929-958.
- 476 34 Zornoff LAM, Paiva SAR, Duarte DR & Spadaro J. Remodelação Ventricular Pós-
477 Infarto do Miocárdio: Conceitos e Implicações Clínicas. *Arq Bras Cardiol*. 2009; 92: 157-
478 164.
- 479 35 Yang F, Li P, Li H, Shi Q, Li S & Zhao L. microRNA-29b Mediates the Antifibrotic
480 Effect of Tanshinone IIA in Postinfarct Cardiac Remodeling. *J Cardiovasc Pharmacol*.
481 2015; 65: 456-64.

- 482 36 Wang JH, Su F, Wang S, et al. CXCR6 deficiency attenuates pressure overload-
483 induced monocytes migration and cardiac fibrosis through downregulating TNF- α -
484 dependent MMP9 pathway. *Int J Clin Exp Pathol*. 2014; 7: 6514-23.
- 485 37 Wang Q, Yu X, Xu H, Zhao X, Sui D, Re G. Improves Isoproterenol-Induced
486 Myocardial Fibrosis and Heart Failure in Rats, Evidence-Based Complem and Alternat
487 Med. 2019; 1-9.
- 488 38 Lindner D, Zietsch C, Tank J, et al. Cardiac fibroblasts support cardiac inflammation
489 in heart failure. *Basic Res Cardiol*. 2014; 109: 428.
- 490 39 Souza RWA, Fernandez GJ, Cunha JPQ, et al. Regulation of cardiac microRNAs
491 induced by aerobic exercise training during heart failure. *Am J Physiol Heart CircPhysiol*.
492 2015; 309: 1629-1641.
- 493 40 Agarwal D, Haque M, Sriramula S, Mariappan N, Pariaut R, Francis J. Role of
494 proinflammatory cytokines and redox homeostasis in exercise-induced delayed
495 progression of hypertension in spontaneously hypertensive rats. *Hypertension*. 2009; 54:
496 1393–1400.
- 497 41 McMullen JR & Jennings GL. Differences between pathological and physiological
498 cardiac hypertrophy: novel therapeutic strategies to treat heart failure. *Clin Exp*
499 *Pharmacol Physiol*. 2007; 34: 255–262.
- 500 42 Soci UP, Fernandes T & Hashimoto NY. MicroRNAs 29 are involved in the
501 improvement of ventricular compliance promoted by aerobic exercise training in rats.
502 *Physiol Genomics*. 2011; 43: 665-73.

503 43 Kwak HB, Kim JH, Joshi K, Yeh A, Martinez DAn & Lawler JM. Exercise training
504 reduces fibrosis and matrix metalloproteinase dysregulation in the aging rat heart. *Faseb*
505 *J.* 2011; 25: 1106-17.

506 44 Xu X & Wan W. Effects of exercise training on cardiac function and myocardial
507 remodeling in post myocardial infarction rats. *J Mol Cell Cardiol.* 2008; 44: 114-22.

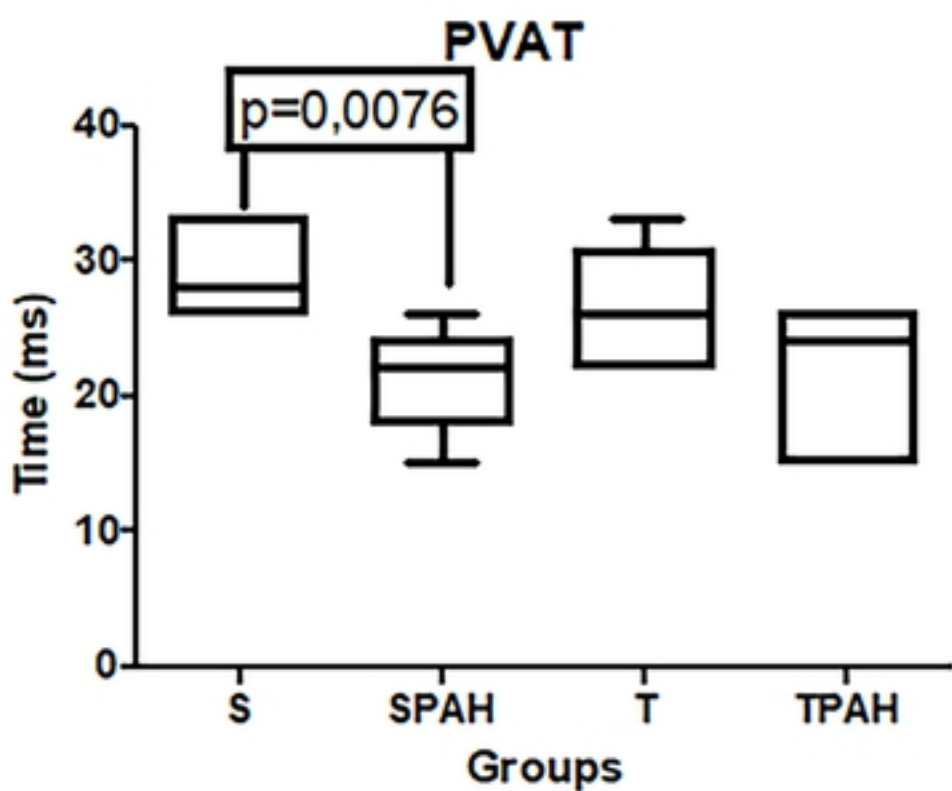
508 45 Nunes RB, Alves JP, Kessler LP & Dal Lago P. Aerobic exercise improves the
509 inflammatory profile correlated with cardiac remodeling and function in chronic heart
510 failure rats. *Clinics.* 2013; 68: 876-82.

511 46 Alves JP, Nunes RB, Stefani GP & Dal Lago P. Resistance training improves
512 hemodynamic function, collagen deposition and inflammatory profiles: experimental
513 model of heart failure. *PLoS One.* 2014; 9: e110317.

514 **Funding**

515 This study was supported by grants 2016/11344-0, 2018/12526-0 and 2018/24317-7 São Paulo
516 Research Fondation (FAPESP).

517

A

bioRxiv preprint doi: <https://doi.org/10.1101/2020.12.17.423207>; this version posted December 17, 2020. The copyright holder for this preprint (which was not certified by peer review) is the author/funder, who has granted bioRxiv a license to display the preprint in perpetuity. It is made available under aCC-BY 4.0 International license.

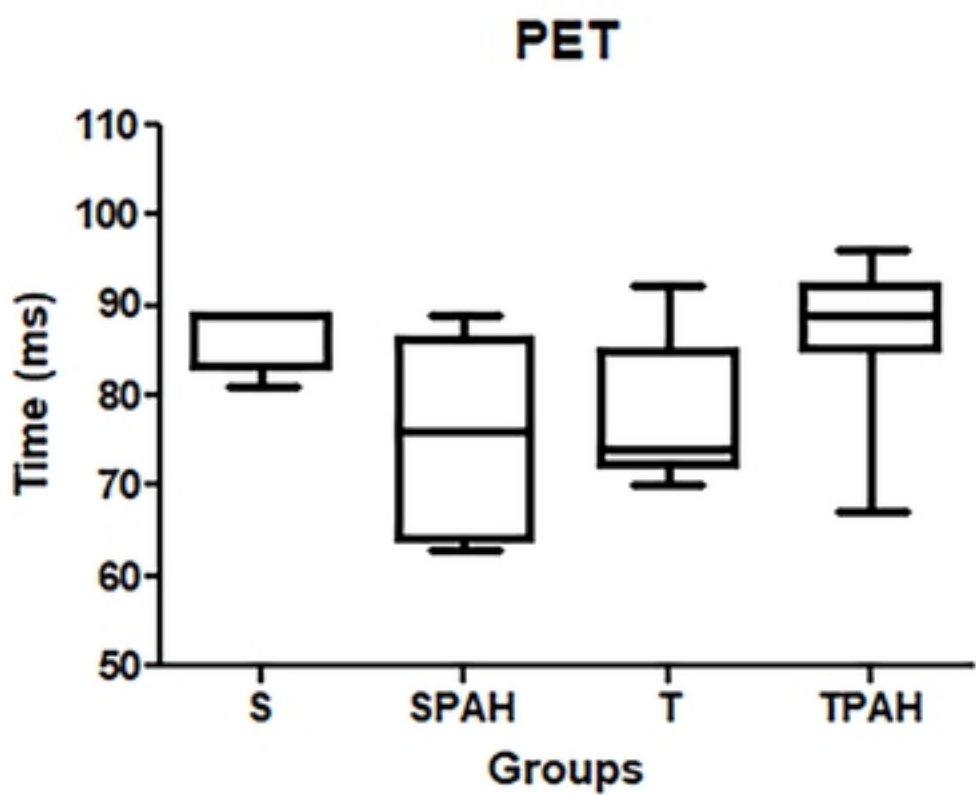
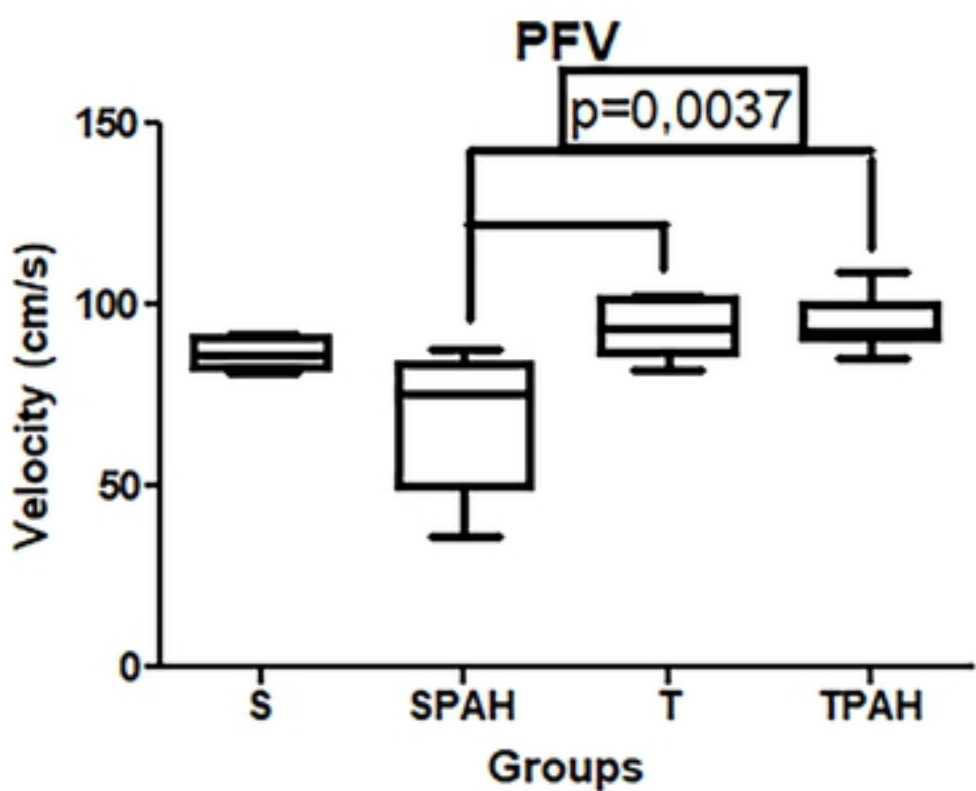
B**C**

Figure 1

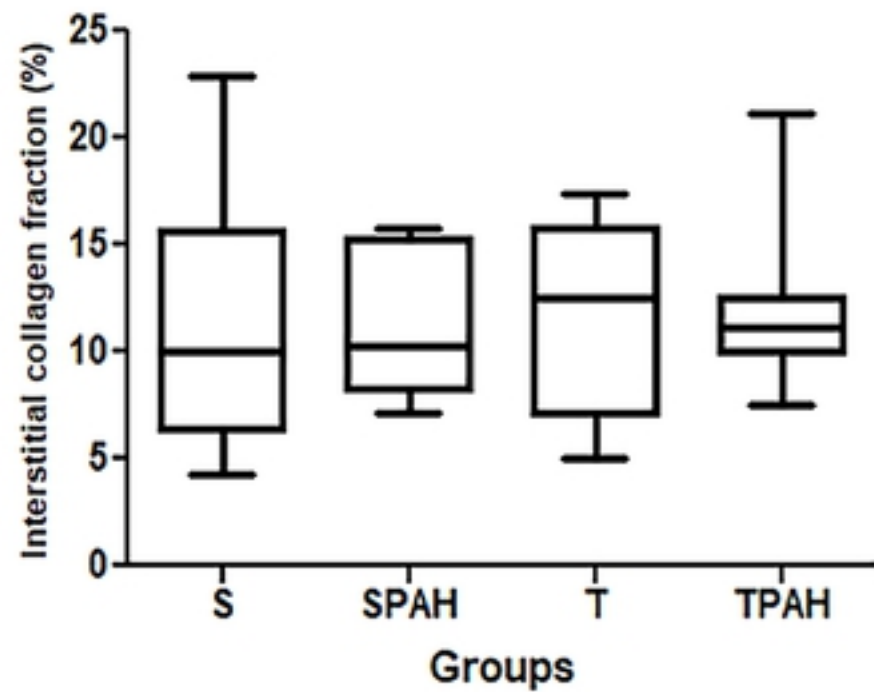
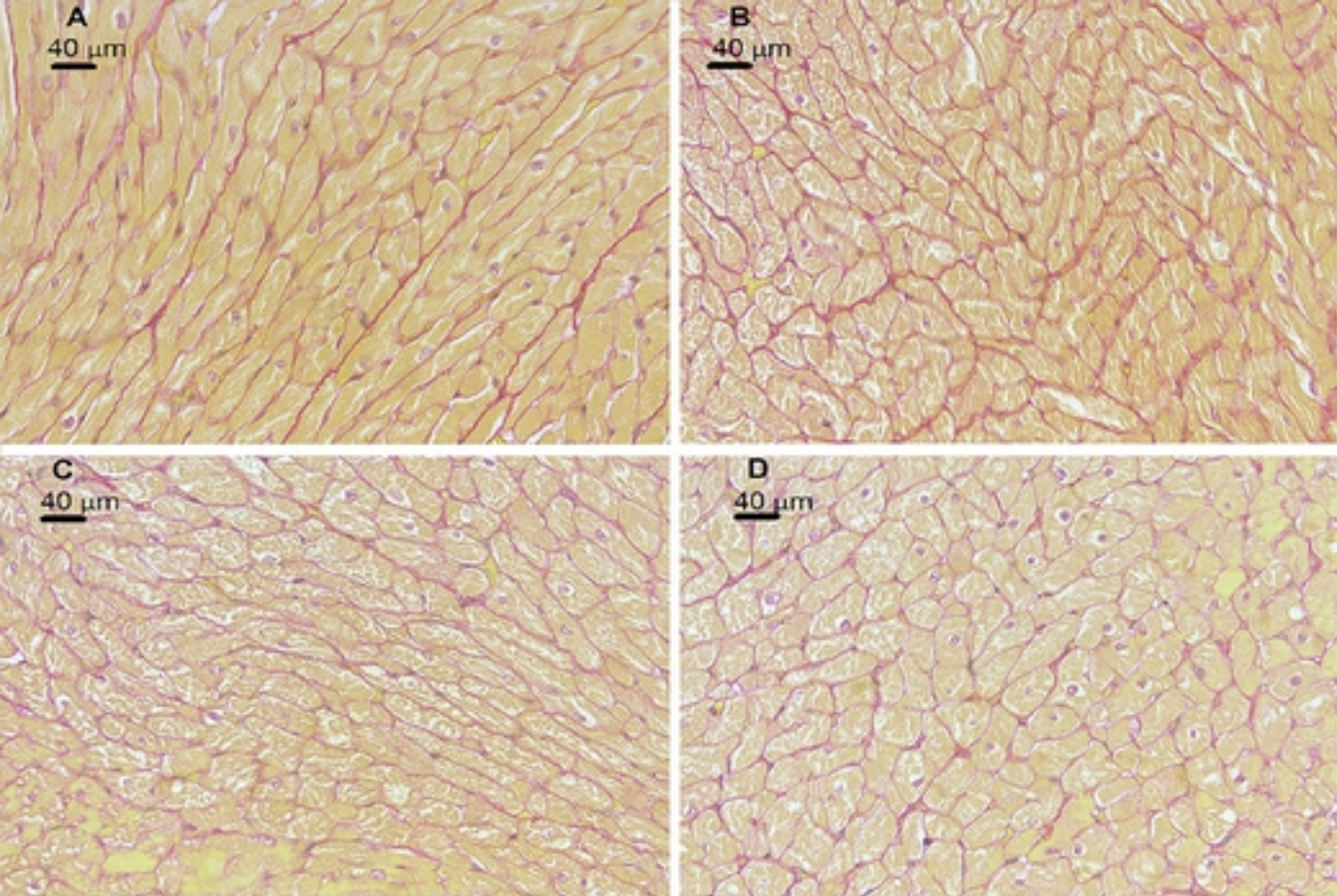


Figure 2

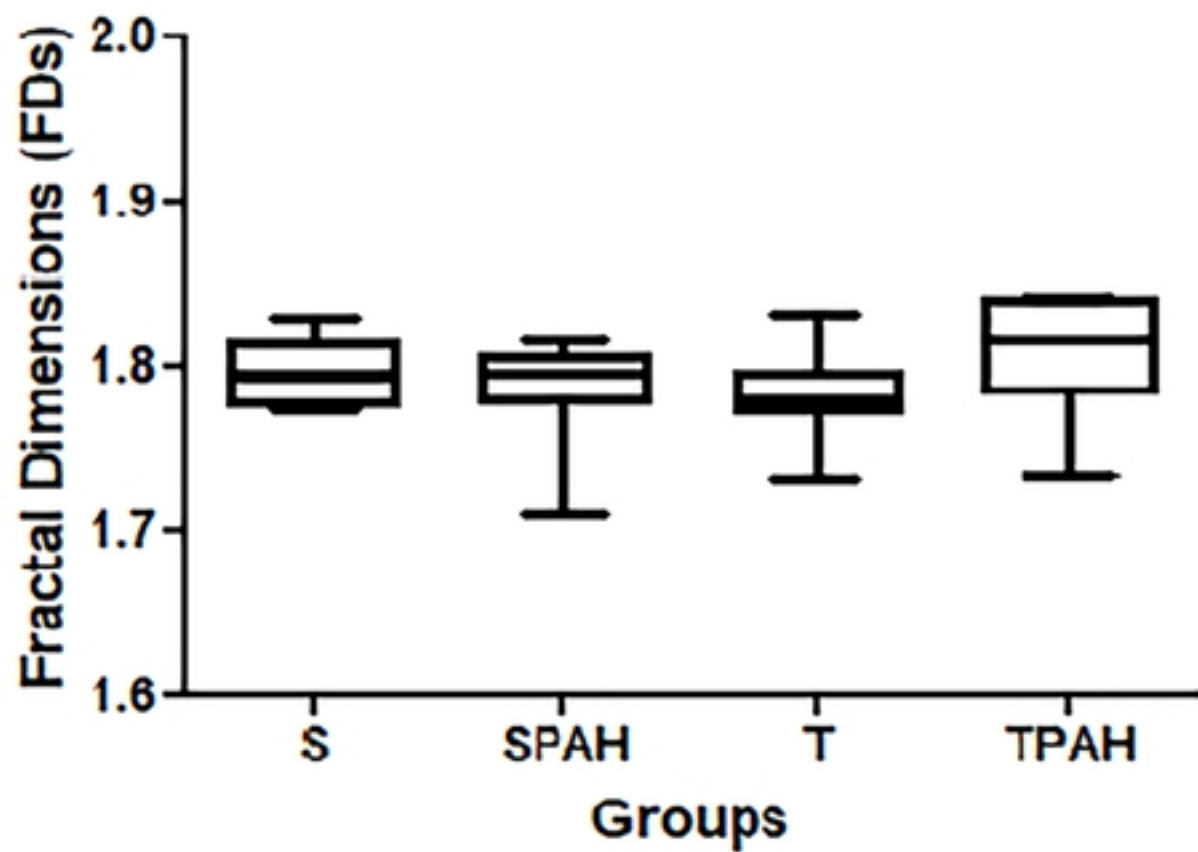
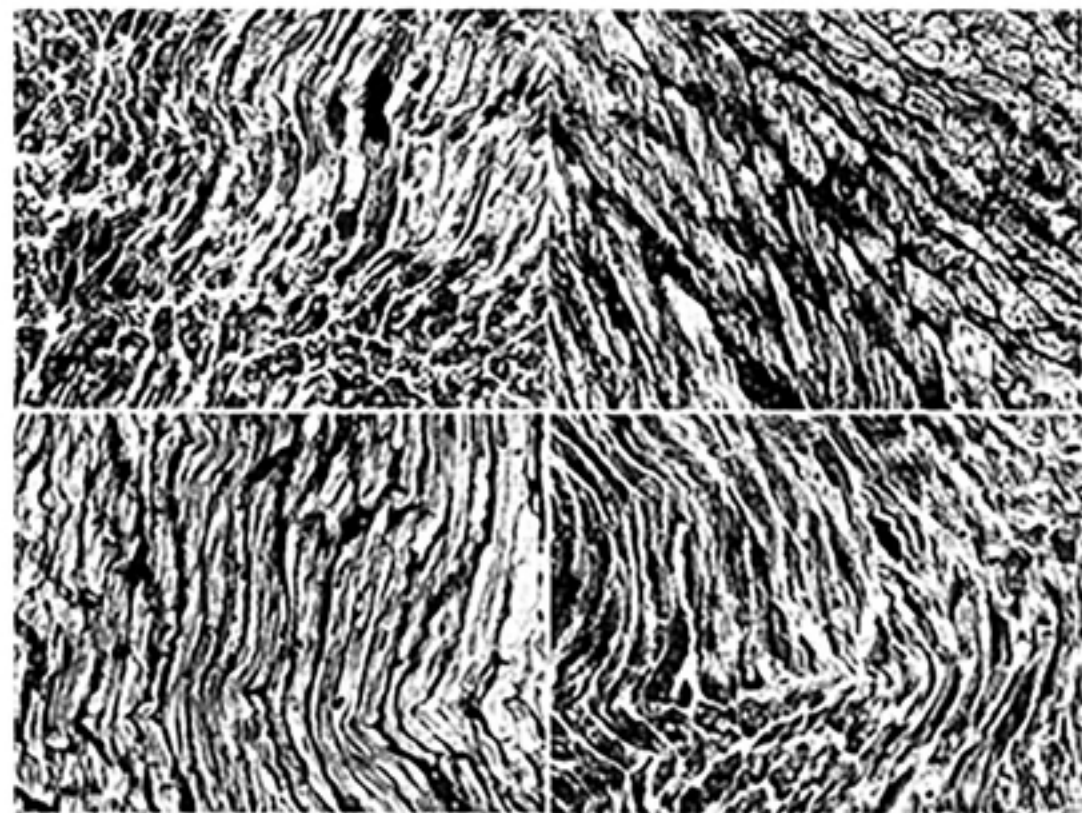


Figure 3

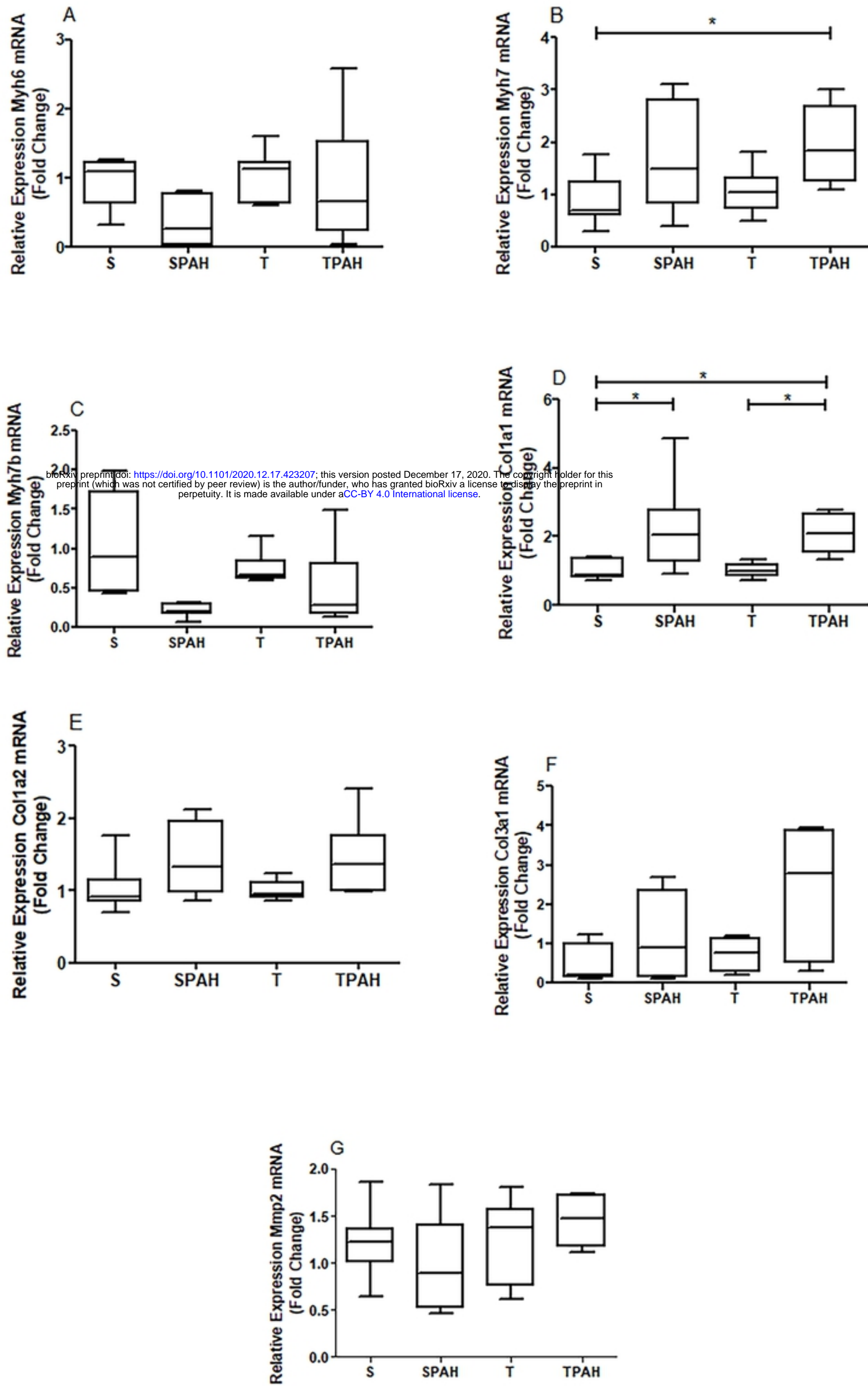


Figure 4